

# Quantum tunneling in a three dimensional network of exchange coupled single-molecule magnets

R. Tiron<sup>1</sup>, W. Wernsdorfer<sup>1</sup>, N. Aliaga-Alcalde<sup>2</sup>, D.N. Hendrickson<sup>3</sup>, G. Christou<sup>2</sup>

<sup>1</sup>Lab. L. Néel, associé à l'UJF, CNRS, BP 166, 38042 Grenoble Cedex 9, France

<sup>2</sup>Dept. of Chemistry, Univ. of Florida, Gainesville, Florida 32611-7200, USA

<sup>3</sup>Dept. of Chemistry and Biochemistry, Univ. of California at San Diego, La Jolla, California 92093-0358, USA

(Dated: January 9, 2022)

A  $\text{Mn}_4$  single-molecule magnet (SMM) is used to show that quantum tunneling of magnetization (QTM) is not suppressed by moderate three dimensional exchange coupling between molecules. Instead, it leads to an exchange bias of the quantum resonances which allows precise measurements of the effective exchange coupling that is mainly due to weak intermolecular hydrogen bounds. The magnetization versus applied field was recorded on single crystals of  $[\text{Mn}_4]_2$  using an array of micro-SQUIDs. The step fine structure was studied via minor hysteresis loops.

PACS numbers: 75.45.+j, 75.60.Ej, 75.50.Xx

Single-molecule magnets (SMM), such as  $\text{Mn}_{12}$ ,  $\text{Mn}_4$  and  $\text{Fe}_8$  [1, 2, 3, 4, 5], have become model systems to study quantum tunneling of magnetization (QTM) [6, 7, 8, 9, 10, 11]. These molecules comprise several magnetic ions, with their spins coupled by strong exchange interactions to give a large effective spin. The molecules are regularly assembled in large crystals where often all the molecules have the same orientation. Hence, macroscopic measurements can give direct access to single molecule properties. Many non-magnetic atoms surround the magnetic core of each molecule. Exchange interactions between molecules are therefore relatively weak and have been neglected in most studies.

Recently, the study of a dimerized SMM  $[\text{Mn}_4]_2$  showed that intermolecular exchange interactions are not negligible [12]. This compound belongs to the  $[\text{Mn}_4\text{O}_3\text{Cl}_4(\text{O}_2\text{CR})_3(\text{py})_3]_2$  family, with  $\text{R} = \text{CH}_2\text{CH}_3$  and it will be named in the following as compound **1**. The spins of the two  $\text{Mn}_4$  molecules are coupled antiferromagnetically. Each molecule acts as a bias on its neighbor, the quantum tunneling resonances thus being shifted with respect to the isolated SMM. In this letter we show that even in three-dimensional networks of exchange coupled SMMs, ordering effects do not quench tunneling.

We selected a dimerized SMM  $[\text{Mn}_4]_2$ , called compound **2**. The molecule belongs to the same family as compound **1**, however  $\text{R} = \text{CH}_3$ . Because this substituent has a smaller volume than  $\text{R} = \text{CH}_2\text{CH}_3$ , molecules are packed closer together. This leads to stronger interdimer interactions, which are negligible in compound **1**. The preparation, X-ray structure and detailed physical characterization have been reported elsewhere [13, 14]. Compounds **1** and **2** crystallize in the hexagonal space group  $R\bar{3}(\text{bar})$  with two  $\text{Mn}_4$  molecules per unit cell lying head-to-head on a crystallographic  $S_6$  symmetry axis (Fig. 1). Each monomer  $\text{Mn}_4$  has a ground state spin  $S = 9/2$ . The Mn-Mn distances and the Mn-O-Mn angles are similar and the uniaxial anisotropy

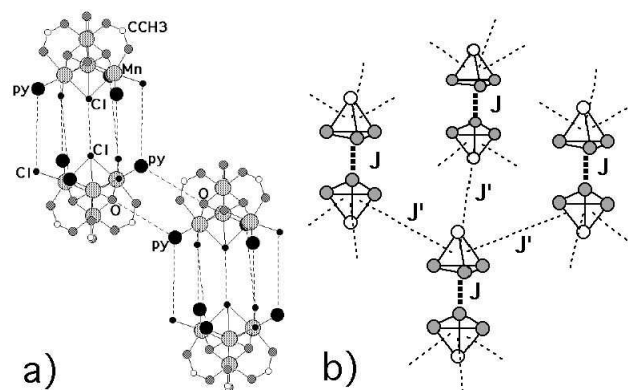


FIG. 1: (a) X-ray crystal structure of the  $\text{Mn}_4$  molecule; the two molecules of a dimer are held together by six hydrogen bonds (3.6 Å) between the pyridine rings (py) and the Cl ions, and one Cl...Cl van der Waals bond (3.74 Å). Two neighboring dimers interact via two hydrogen bonds (3.23 Å) between the py and the O ion. (b) Schematic view of the exchange coupled network of  $\text{Mn}_4$  molecules. Each  $\text{Mn}_4$  molecule (schematized by the  $\text{Mn}_4$  tetrahedron), is exchange coupled to the  $\text{Mn}_4$  of the dimer ( $J$ ) and to three molecules of nearby dimers ( $J'$ ).

constant is expected to be the same for the two dimer systems. These dimers are held together via six  $\text{C}-\text{H} \cdots \text{Cl}$  hydrogen bonds between the pyridine (py) rings on one molecule and the Cl ions on the other and one  $\text{Cl} \cdots \text{Cl}$  Van der Waals interaction (Fig. 1a). These interactions lead to an antiferromagnetic superexchange interaction between the two  $\text{Mn}_4$  units of a dimer [12].

Owing to the  $S_6$  symmetry of  $[\text{Mn}_4]_2$ , each  $\text{Mn}_4$  is close to three neighboring  $\text{Mn}_4$  molecules of the three neighboring  $[\text{Mn}_4]_2$  (Fig. 1b). There are hydrogen bonds between the pyridine (py) rings of the molecules and the O ions of the other three neighboring molecules. The  $\text{C}-\text{H} \cdots \text{O}$  hydrogen bonds between  $[\text{Mn}_4]_2$  dimers have  $\text{C} \cdots \text{O}$  distances and  $\text{C}-\text{H} \cdots \text{O}$  angles of 4.05 Å and  $124.85^\circ$ , respectively. The interactions between the dimers are expected to be antiferromagnetic and weaker

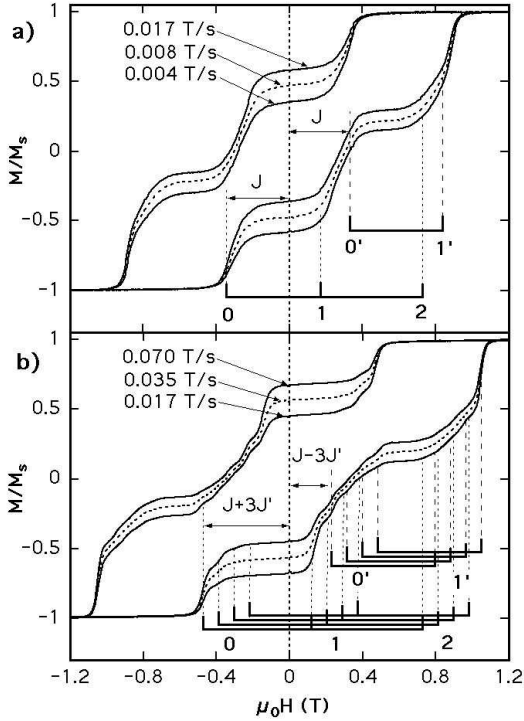


FIG. 2: Hysteresis loops for compounds **1** (a) and **2** (b), measured at different sweep rates. If the spin of one molecule is in the  $-9/2$  state, the resonance positions of the other molecule are shifted towards negative fields. The comb (0,1,2) represents the resonances of one molecule from  $-9/2$  to  $+9/2$  (0), from  $-9/2$  to  $+7/2$  (1), and from  $-9/2$  to  $+5/2$  (2). If the spin of the other molecule is in the  $+9/2$  states, the resonances are shifted towards positive fields, indicated by the comb (0',1'). The step fine structure of compound **2** is explained by exchange coupling with neighbors. It can be explained by the splitting of each comb into four combs (Fig. 2b).

than the interdimer interactions. The two different antiferromagnetic couplings, the stronger one inside the dimer and the weaker one between the dimers, make this system an interesting candidate for studying the QTM in a three dimensional network of exchange coupled SMMs.

The magnetization versus applied field was recorded on single crystals of  $[\text{Mn}_4]_2$  using an array of micro-SQUIDS [15]. Figs. 2a and 2b show typical hysteresis loops of magnetization versus applied field for different field sweep rates. The field is applied along the easy axis of magnetization of a single crystal of about  $20\text{ }\mu\text{m}$ . These loops display step-like features separated by plateaus. The hysteresis loops of the two crystals are similar. However, compound **2** shows a fine structure that is absent in the hysteresis loops of compound **1**. We will show in the following that the main feature of the hysteresis loops can be explained by the QTM of one  $\text{Mn}_4$  molecule, coupled by a superexchange interaction  $J$  to the other unit of the  $[\text{Mn}_4]_2$  dimer. We discuss

first compound **1** because the coupling with neighboring dimers can be neglected [12]. Then, we show that the fine structure observed for compound **2** is induced by a superexchange interaction  $J'$  between neighboring dimers (Fig. 1b).

The simplest Hamiltonian describing the spin system of an isolated SMM is:

$$\mathcal{H} = -DS_z^2 + \mathcal{H}_{\text{trans}} + g\mu_B\mu_0\vec{S} \cdot \vec{H} \quad (1)$$

$S_x$ ,  $S_y$ , and  $S_z$  are the components of the spin operator;  $D$  is the anisotropy constant defining an Ising type of anisotropy;  $\mathcal{H}_{\text{trans}}$ , containing  $S_x$  or  $S_y$  spin operators, gives the transverse anisotropy which is small compared to  $DS_z^2$  in SMMs; and the last term describes the Zeeman energy associated with an effective field  $\vec{H}$ . For one isolated spin the effective field is the applied field. This Hamiltonian has an energy level spectrum with  $(2S+1)$  values which, to a first approximation, can be labelled by the quantum numbers  $M = -S, -(S-1), \dots, S$  taking the  $z$ -axis as the quantization axis. The energy spectrum can be obtained by using standard diagonalization techniques. At  $\vec{H} = 0$ , the levels  $M = \pm S$  have the lowest energy. When a positive field  $H_z$  is applied, the levels with  $M > 0$  decrease in energy, while those with  $M < 0$  increase. Therefore, energy levels of positive and negative quantum numbers cross at certain values of  $H_z$  given by  $\mu_0 H_z \approx nD/g\mu_B$ , where  $n = 0, 1, 2, 3, \dots$ . When the spin Hamiltonian contains transverse terms ( $\mathcal{H}_{\text{trans}}$ ), the level crossings can be *avoided level crossings*. The spin  $S$  is *in resonance* between two states when the local longitudinal field is close to an avoided level crossing. The energy gap, the so-called *tunnel splitting*  $\Delta$ , can be tuned by a transverse field (a field applied perpendicular to the  $z$  direction) via the  $S_x H_x$  and  $S_y H_y$  Zeeman terms. The effect of these avoided level crossings leads to well defined steps in hysteresis loop measurements.

The main point to note is that the giant spin Hamiltonian predicts always the first level crossing at zero field, corresponding to the QTM of a SMM between  $M = \pm S$  states. Thus, for compound **1** (see Fig. 2a), the single-spin Hamiltonian is not sufficient to explain the first resonance shifted to negative fields and the absence of the quantum tunnelling at zero field, in contrast to other SMMs.

In order to explain the observed features in Fig. 2a, one has to take into account the superexchange coupling  $J$  between pairs of  $\text{Mn}_4$  units. A Hamiltonian for the two-coupled molecules can be written and the energy states of the  $[\text{Mn}_4]_2$  can be calculated by exact diagonalization. More details on the dimer Hamiltonian and the corresponding Zeeman diagram are reported elsewhere [12]. Here, we propose a phenomenological model that is sufficiently simple to allow inclusion, in a second step, of more exchange couplings. The influence of the exchange coupling of the neighboring molecule is taken into account

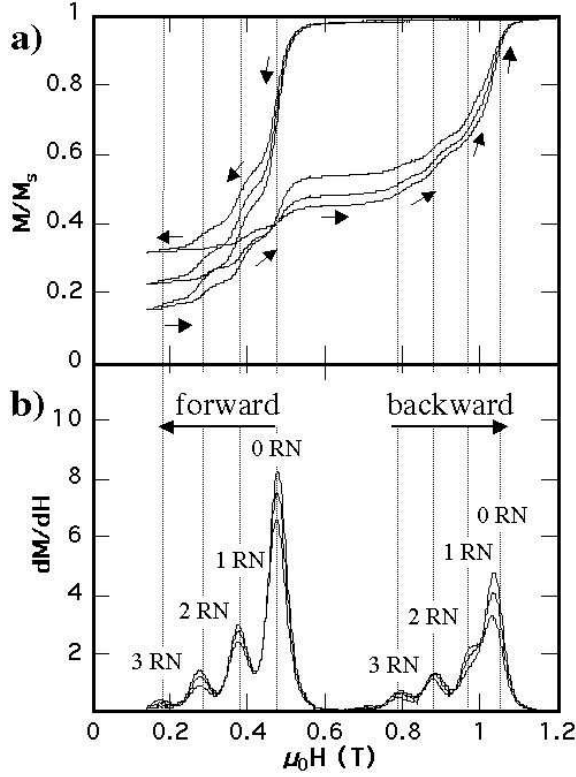


FIG. 3: Field sweep rate dependence of (a) the minor hysteresis loops and (b) the derivatives of the hysteresis loops, measured on a single crystal of compound **2** at 0.04 K. The positions corresponding to 0, 1, 2, or 3 reversed neighbors (RN) are indicated.

by an exchange bias field  $H_{bias}$ . The effective field  $H_z$  acting on the molecule is therefore the sum of the applied field  $H_{app}$  and the bias field  $H_{bias}$ :

$$H_z = H_z^{app} + H_z^{bias} = H_z^{app} + \frac{J}{g\mu_B\mu_0} M_2 \quad (2)$$

where  $M_2$  is the quantum number of the neighboring molecule and  $J$  is the associated exchange coupling. In the following we explain the hysteresis loops when the field  $H_z^{app}$  is swept from negative to positive values. At low temperature,  $M_2$  has two possible values  $M_2 = \pm S = \pm 9/2$ . We expect therefore resonant QTM for applied fields  $\mu_0 H_z^{app} \approx nD/g\mu_B \pm M_2 J/g\mu_B$ , where  $n = 0, 1, 2, 3, \dots$ . The two possibilities of  $M_2$  are represented by two combs in Fig. 2a. The first comb (0,1,2) corresponds to  $M_2 = -9/2$  and the second one (0',1') to  $M_2 = 9/2$ . This model describes all observed quantum transitions in Fig. 2a with two fitting parameters  $D/k_B = -0.72$  K and  $J/k_B = 0.1$  K. It neglects co-tunneling and other two-body tunnel transitions having a lower probability of occurrence [12, 16].

Compound **2** displays hysteresis loops (Fig. 2b) similar to those of compound **1**. However, the total exchange coupling is larger for compound **2**. The values of

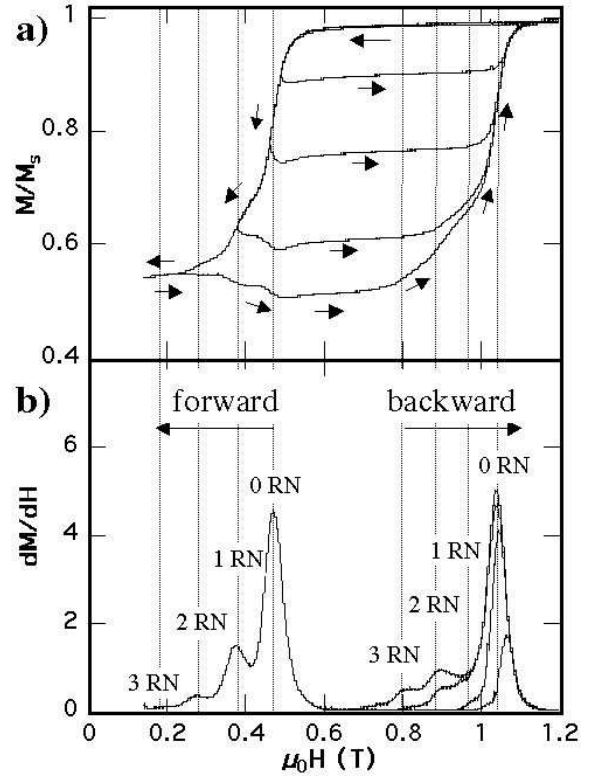


FIG. 4: (a) Several minor hysteresis loops and (b) their derivatives, measured on a single crystal of compound **2** at 0.04 K. The field sweep rate is 0.14 T/s. The positions corresponding to 0, 1, 2, or 3 reversed neighbors (RN) are indicated.

$D/k_B = -0.75$  K and  $J/k_B = 0.15$  K were obtained from the field positions of the steps in the hysteresis loops. Another difference between the two compounds is that the hysteresis loops of compound **2** exhibit fine structure that can not be explained by the dimer model described above (Eq. 2). In order to better analyze this fine structure, minor hysteresis loops were measured (Figs. 3 and 4). First the sample is saturated in positive field; all the molecules are in the  $M = +9/2$  state. Then the field is decreased. The system approaches the first avoided energy level crossing at a field value of  $\approx 0.5$  T. A fraction of the dimers switches from  $+9/2$  to  $-9/2$ , and the total magnetization of the system decreases, generating a step in the hysteresis loop. When the magnetization reaches the second plateau ( $\approx 0.2$  T), the field is swept back towards positive saturation; the tunneling from  $M = -9/2$  to  $9/2$  is favored via the excited state  $7/2$  ( $\approx 1$  T). After this transition the sample reaches positive saturation. The purpose of these minor hysteresis loops is to confirm the fine structure of each transition starting from different initial states.

The tunnel transitions exhibit four equidistant kinks, that we explain by the exchange coupling to the three neighboring dimers. The spin of the three neighboring

molecules can be either aligned with the magnetic field or reversed, leading to four different situations: from zero to three reversed neighbors.

The exchange coupling between a molecule and its neighbors acts like a supplementary field bias and shifts further the resonance fields. The total field bias induced by the neighbors and the other  $\text{Mn}_4$  unit of the dimer can be written:

$$H_{\text{bias}}^{\text{tot}} = \frac{1}{g\mu_B\mu_0} \left( JM_2 + \sum_{i=1}^3 J' M'_i \right) \quad (3)$$

where the first term is the contribution of the intradimer coupling, and  $M'_i$  is the quantum number of the three neighboring dimer molecules  $i$  (Fig. 1b).

After positive saturation all the molecules are aligned with the field. The first kink in the hysteresis loop corresponds to the QTM of one molecule in the bias field of its non-reversed neighbors. The resonance is shifted towards negative values by the bias field  $H_{\text{bias}} = 9/(2g\mu_B\mu_0)(J + 3J')$  (see Eq.4). After this first kink, some molecules now have one reversed neighbor. At the second kink it is this newly created population which tunnels generating molecules with two reversed neighbors. The corresponding field shift is  $H_{\text{bias}} = 9/(2g\mu_B\mu_0)(J + J')$ . The third and the fourth kinks are generated by the QTM of molecules having, respectively, two and three reversed neighbors. The field shift between two consecutive kinks is  $\approx 0.1$  T, corresponding to an interdimer interaction  $J' \approx 0.015$  K.

Minor hysteresis loops were measured for different field sweep rates (Fig. 3) and reversal fields (Fig. 4) in order to probe the step heights of the fine structure: the smaller the sweep rate the higher the resulting kink. This dependence is justified by the Landau Zener model. The main point to note is that heights of two consecutive kinks are correlated. The second kink height is smaller than the first kink height, the third smaller than the second, and so on. This result is in good agreement with our model: in order to have quantum tunneling of molecules with  $n$  reversed neighbors, the  $n$  neighbors must have previously reversed.

All the other transitions exhibit the same kind of fine structure, which can be explained by the above model leading to the 8 combs in Fig. 2b, giving for the three

fitting parameters  $D/k_B \approx -0.75$  K,  $J/k_B \approx 0.1$  K and  $J'/k_B \approx 0.015$  K.

The above results demonstrate that a three dimensional network of exchange coupled SMMs doesn't suppress QTM. The intermolecular interactions are strong enough to cause a clear field bias, but too weak to transform the spin network into a *classical* antiferromagnetic material. This three dimensional network of exchange coupled SMMs demonstrate that the QTM can be controlled using exchange interactions, and opens up new perspectives in the use of supramolecular chemistry to modulate the quantum physics of these molecular nanomagnets.

- 
- [1] G. Christou, D. Gatteschi, D.N. Hendrickson, and R. Sessoli, MRS Bulletin **25**, 66 (2000).
  - [2] R. Sessoli, H.-L. Tsai, A. R. Schake, S. Wang, J. B. Vincent, K. Folting, D. Gatteschi, G. Christou, and D. N. Hendrickson, J. Am. Chem. Soc. **115**, 1804 (1993).
  - [3] R. Sessoli, D. Gatteschi, A. Caneschi, and M. A. Novak, Nature **365**, 141 (1993).
  - [4] S. M. J. Aubin and *et al.*, J. Am. Chem. Soc. **118**, 7746 (1996).
  - [5] C. Boskovic and *et al.*, J. Am. Chem. Soc. **124**, 3725 (2002).
  - [6] J. R. Friedman, M. P. Sarachik, J. Tejada, and R. Ziolo, Phys. Rev. Lett. **76**, 3830 (1996).
  - [7] L. Thomas, F. Lioni, R. Ballou, D. Gatteschi, R. Sessoli, and B. Barbara, Nature (London) **383**, 145 (1996).
  - [8] C. Sangregorio, T. Ohm, C. Paulsen, R. Sessoli, and D. Gatteschi, Phys. Rev. Lett. **78**, 4645 (1997).
  - [9] S. M. J. Aubin, N. R. Dilley, M. B. Wemple, G. Christou, and D. N. Hendrickson, J. Am. Chem. Soc. **120**, 839 (1998).
  - [10] S. M. J. Aubin, N. R. Dilley, M. B. Wemple, G. Christou, and D. N. Hendrickson, J. Am. Chem. Soc. **120**, 4991 (1998).
  - [11] W. Wernsdorfer and R. Sessoli, Science **284**, 133 (1999).
  - [12] W. Wernsdorfer, N. Aliaga-Alcalde, D.N. Hendrickson, and G. Christou, Nature **416**, 406 (2002).
  - [13] D. N. Hendrickson and *et al.*, J. Am. Chem. Soc. **114**, 2455 (1992).
  - [14] N. Aliaga-Alcalde, *et al.*, to be published.
  - [15] W. Wernsdorfer, Adv. Chem. Phys. **118**, 99 (2001).
  - [16] W. Wernsdorfer, S. Bhaduri, R. Tiron, D. N. Hendrickson, and G. Christou, Phys. Rev. Lett. **89**, 197201 (2002).